

International Telecommunication Union

ITU-R
Radiocommunication Sector of ITU

Report ITU-R M.2398-0
(10/2016)

**Scenarios and performance of an integrated
MSS system operating in frequency
bands below 3 GHz**

M Series
**Mobile, radiodetermination, amateur
and related satellite services**



International
Telecommunication
Union

Foreword

The role of the Radiocommunication Sector is to ensure the rational, equitable, efficient and economical use of the radio-frequency spectrum by all radiocommunication services, including satellite services, and carry out studies without limit of frequency range on the basis of which Recommendations are adopted.

The regulatory and policy functions of the Radiocommunication Sector are performed by World and Regional Radiocommunication Conferences and Radiocommunication Assemblies supported by Study Groups.

Policy on Intellectual Property Right (IPR)

ITU-R policy on IPR is described in the Common Patent Policy for ITU-T/ITU-R/ISO/IEC referenced in Annex 1 of Resolution ITU-R 1. Forms to be used for the submission of patent statements and licensing declarations by patent holders are available from <http://www.itu.int/ITU-R/go/patents/en> where the Guidelines for Implementation of the Common Patent Policy for ITU-T/ITU-R/ISO/IEC and the ITU-R patent information database can also be found.

Series of ITU-R Reports

(Also available online at <http://www.itu.int/publ/R-REP/en>)

Series	Title
BO	Satellite delivery
BR	Recording for production, archival and play-out; film for television
BS	Broadcasting service (sound)
BT	Broadcasting service (television)
F	Fixed service
M	Mobile, radiodetermination, amateur and related satellite services
P	Radiowave propagation
RA	Radio astronomy
RS	Remote sensing systems
S	Fixed-satellite service
SA	Space applications and meteorology
SF	Frequency sharing and coordination between fixed-satellite and fixed service systems
SM	Spectrum management

Note: This ITU-R Report was approved in English by the Study Group under the procedure detailed in Resolution ITU-R 1.

Electronic Publication
Geneva, 2017

© ITU 2017

All rights reserved. No part of this publication may be reproduced, by any means whatsoever, without written permission of ITU.

REPORT ITU-R M.2398-0

**Scenarios and performance of an integrated MSS system operating
in frequency bands below 3 GHz**

(Question ITU-R 291/4)

(2016)

TABLE OF CONTENTS

	<i>Page</i>
1 Introduction	4
2 Services and system architectures	5
2.1 Possible services	5
2.2 Possible system architecture	6
3 Possible deployment scenarios	8
3.1 Scenario 1 (frequency segmentation)	8
3.2 Scenario 2 (Frequency reuse)	9
3.3 Scenario 3 (Frequency reuse with interference coordination)	10
4 Performance assessment	10
4.1 Interference path	10
4.2 Interference assessment	11
4.2.1 Propagation model	11
4.2.2 Parameters for the satellite component	11
4.2.3 Parameters for the CGCs	12
4.2.4 Interference assessments	13
4.3 Throughput assessment	21
4.3.1 Link performance and impact on SINR	21
4.3.2 Satellite resource availability in CGCs	24
4.3.3 Throughput degradation in the satellite components	26
5 Technical constraints associated with deployments	28
5.1 Large antenna and multi-beam technology	28
5.2 Radio interface techniques	29
5.3 Interworking between the satellite and CGCs	30
6 Technical enablers for performance enhancements	30
6.1 Efficient frequency reuse schemes	30

	<i>Page</i>
6.2 Interference management schemes	31
6.3 Ground based beam-forming schemes.....	32
6.4 Satellite based digital beam-forming and channelizing schemes	33
Attachment – Development of small-scale prototype DBF/channelizer as an example of technical enablers	34
1 Introduction	34
2 Verification of multiple beamforming and sidelobe reduction	35
3 Verification of channelizing (resource re-allocation).....	37

Scope

This Report describes the identification of possible service and system architecture, deployment scenarios, performance, technical constraints and technical enablers of an integrated MSS system operating in frequency bands below 3 GHz.

Abbreviations/Glossary

3GPP	3 rd Generation Partnership Project
AMC	Adaptive modulation and coding
ARQ	Automatic repeat request
ASIC	Application specific integrated circuit
BLER	Block error rate
BMSat	Broadband mobile satellite
CDMA	Code division multiple access
CGC	Complementary ground components
D/C	Down converter
DBF	Digital beam former
EEZ	Exclusive economic zone
EGAL	Enhanced geostationary air link
FDMA	Frequency division multiple access
FPGA	Field programmable gate array
GBBF	Ground based beam forming
GEO	Geostationary earth orbit
GMR-1	GEO mobile radio interface-1
GPS	Global positioning system

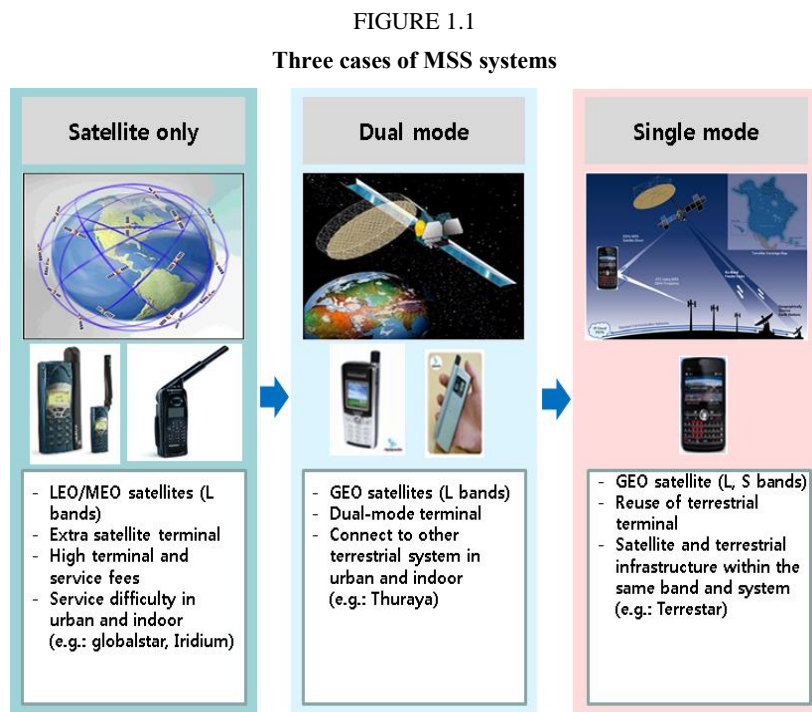
GSM	Global system for mobile communications
GSO	Geosynchronous orbit
HARQ	Hybrid automatic repeat request
HSS	Home subscriber server
IMT	International mobile telecommunications
LEO	Low earth orbit
LNA	Low noise amplifier
LTE	Long term evolution
MCS	Modulation and coding scheme
MEO	Medium earth orbit
MES	Mobile earth station
MME	Mobility management entity
MMS	Multimedia messaging service
MS	Mobile service
MSS	Mobile satellite service
OFDM	Orthogonal frequency division multiplexing
P-GW	Packet data network gateway
PCRF	Policy & charging rules function
PDN	Packet data network
PDU	Protocol data unit
PPDR	Public protection and disaster relief
PUSCH	Physical uplink shared channel
RB	Resource block
S-GW	Serving gateway
SAT	Satellite
SAT-OFDM	Satellite orthogonal frequency division multiplexing
SGIPS	Satellite/ground interworking policy server
SINR	Signal to interference plus noise ratio
SMS	Short message service
SRI	Satellite radio interface
SSPA	Solid state power amplifier
U/C	Up converter
UE	User equipment
VoIP	Voice over Internet Protocol
W-CDMA	Wideband code division multiple access

1 Introduction

Integrated mobile-satellite service (MSS) systems and hybrid satellite/terrestrial systems are innovative space/terrestrial infrastructure with a high degree of spectrum utilization efficiency and have the ability to provide a variety of benefits that serve the public interest, including multimedia broadband services to handheld or portable terminals and public protection and disaster relief (PPDR) solutions, as well as MSS operators from economic viability and economies of scale perspectives.

MSS systems can provide ubiquitous connectivity through their wide-area coverage characteristics and offer instant and reliable communication systems within their coverage area. Their strength and utility in providing blanket coverage to terrestrial communications networks in areas where population densities cannot support introduction of large-scale commercial land-based infrastructure has made MSS systems an indispensable part of communication networks. Terrestrial-based networks on the other hand, have their strength and traditional role in providing high capacity communication networks in suburban and urban areas, including inside buildings, that no conventional MSS system has the ability to penetrate due to excessive blockage and shadowing of the satellite link in such areas.

Figure 1.1 shows the development trends of MSS systems.

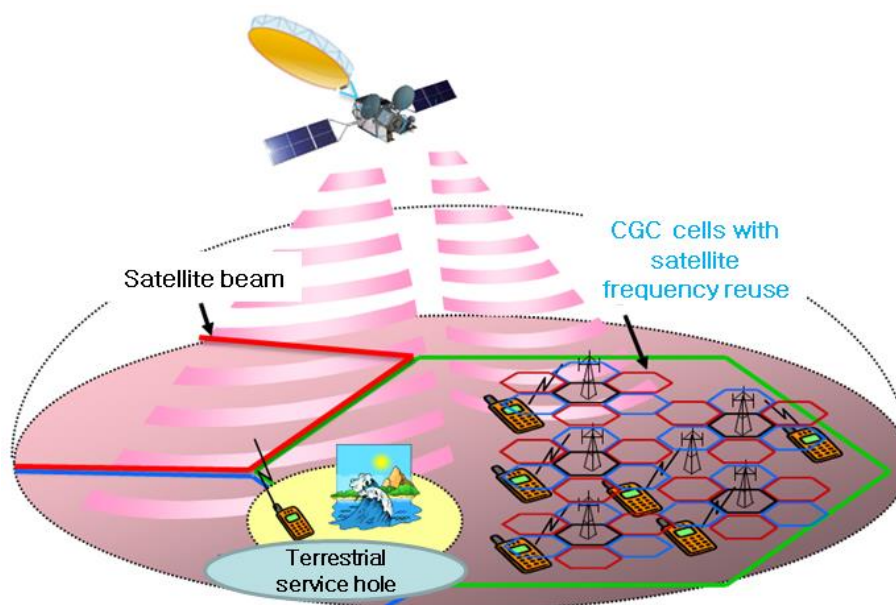


In the context of the drive to deliver broadband services throughout global coverage, the MSS system will promote the rapid deployment and delivery of such services to rural areas, geographically isolated areas and countries where wire-line networks are still in need of significant upgrading before wire-line broadband is achievable. In those rural areas where broadband is already or is soon to be available, the deployment of MSS broadband services will provide an alternative service, thereby promoting choice. In addition, the implementation of complementary ground components (CGCs) in a MSS system could allow for the development of a range of new market and broadband services. The CGCs will operate at the same frequencies as the associated satellites and be used to improve the availability of MSS, for example in areas where the communication with space stations cannot be guaranteed. The CGCs will provide more efficient spectrum usage and improved coverage according to the deployment of the CGCs would further attract larger

consumer markets resulting in increased economies of scale. This will make the costs of producing handsets and overall price of the services to end users reduced, ensuring that the cost of MSS in remote areas should be reduced remarkably.

Figure 1.2 shows the concept of an integrated satellite and terrestrial communication. In many regions, satellite operators are allowed to deploy CGCs in order to improve the satellite service coverage. Broadband services such as IMT is provided into single mode UE (quasi-terrestrial IMT UE) through one of satellite and terrestrial components operating within the satellite frequency bands. In those integrated MSS systems, one of the key issues is how to optimize the spectral efficiency of the MSS system as a whole (satellite plus CGC).

FIGURE 1.2
Concept of an integrated MSS system



CGCs are different from independent ground components used by MS operators as they are technically and operationally an integral part of the satellite system and are controlled by the common resource and network management mechanism of such system operating in the same frequencies as the associated satellite components and being delivered to an integrated user equipment.

2 Services and system architectures

2.1 Possible services

Major advantages of infrastructure based on integrated MSS system composed of satellite and ground components would be as follows:

- Service coverage extension (e.g. maritime, rural and low density populated areas).
- A wide range of service provisioning with low cost for both customers and operators.
- (Rapid) infrastructure independent service deployment (e.g. backhaul solution).

Possible services using integrated MSS systems are as follows. Satellite component in the integrated MSS system will provide the service with similar quality to those of CGC.

- Messaging (SMS, MMS, email, etc.).

- Voice telephony (including VoIP).
- High quality video telephony.
- Push-to-talk.
- Video conference (including high quality).
- Internet browsing.
- Interactive game.
- File transfer/download.
- Multimedia.
- E-education.
- Consultation.
- Remote collaboration.
- Mobile commerce.
- Mobile broadcasting/multicasting.
- Machine-to-machine communication.
- Remote sensor.
- Remote bio-monitoring.
- Personal environment service.
- ITS-enabled services.
- Emergency calling.
- Public alert.
- Location based service.

2.2 Possible system architecture

Figure 2.1 shows the general system architecture for the integrated MSS system. The system consists of satellite and CGC, operating in the MSS bands in a way that CGC can reuse satellite frequencies which are used for adjacent satellite beams. Satellite management system should make efficient resource allocations (frequency, subcarrier, power, etc.) for CGCs for optimized system deployment by maximizing overall system throughput under satisfying service requirements of both components. SAT/CGC gateway can decide which component is appropriate for packet transmission considering the situations of satellite and CGC network.

FIGURE 2.1

Overall system architecture

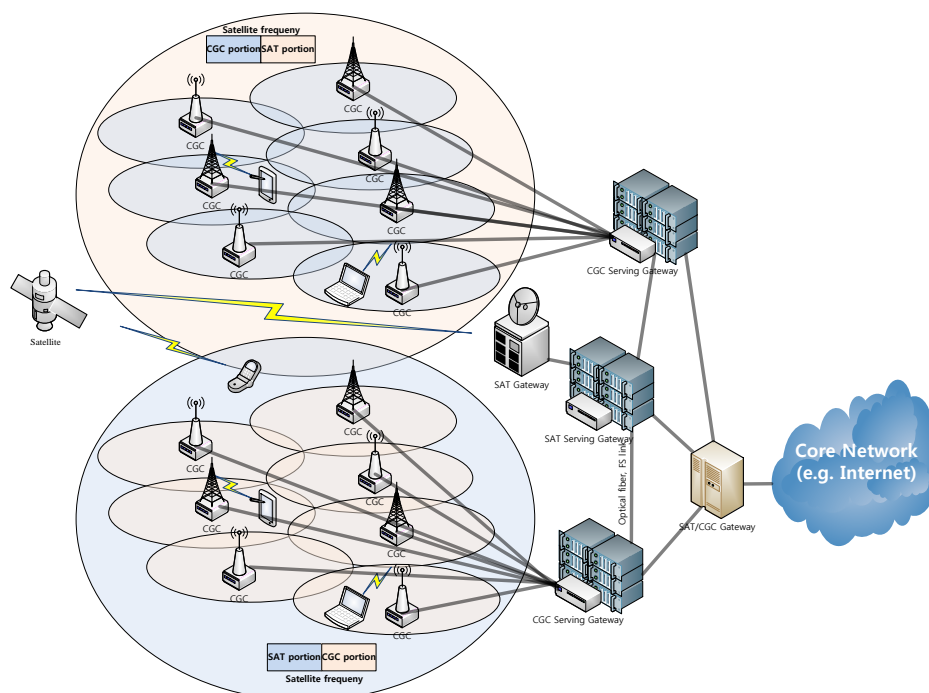
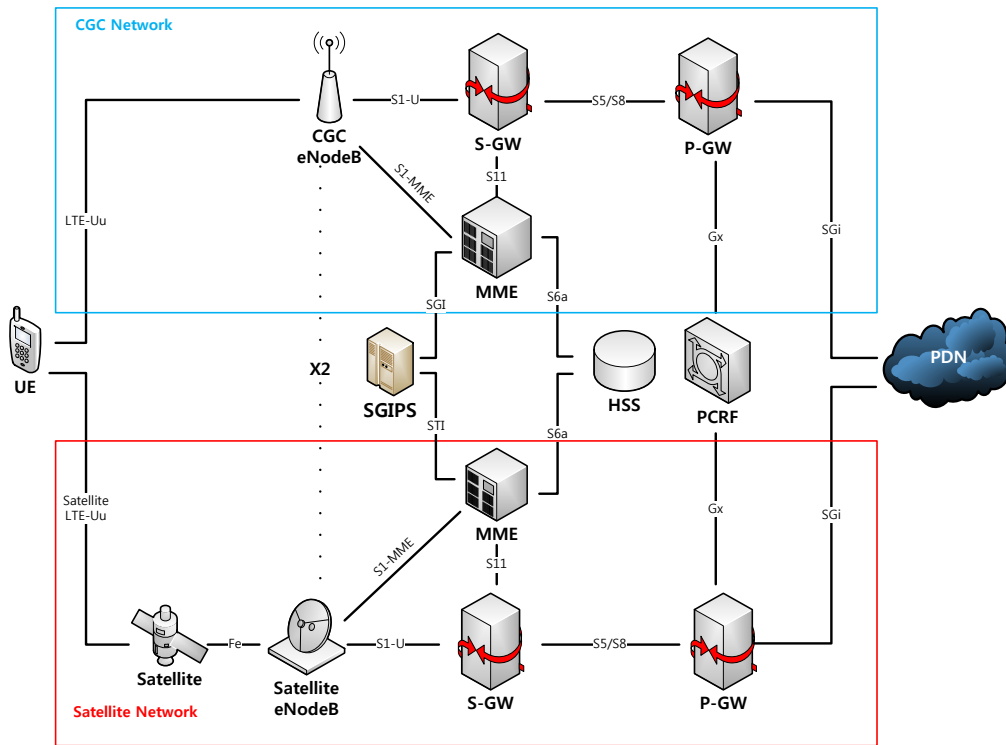


Figure 2.2 represents one example of overall network architecture based on 3GPP long-term evolution (LTE) protocol to implement the overall system architecture as in Fig. 2.1.

For cost-effective deployment, LTE based network architecture needs to be adapted into the satellite component. That is, the satellite network consists of eNodeB for satellite radio interface, serving gateway (S-GW), mobility management entity (MME), home subscriber server (HSS), policy & charging rules function (PCRF) and packet data network (PDN) gateway (P-GW). Furthermore, the SAT-OFDM and BMSat radio interface technologies, which are included in Recommendation ITU-R M.2047 regarding the detailed specification for the satellite radio interface of IMT-Advanced, could be considered for this LTE based satellite network.

FIGURE 2.2

Network architecture for LTE based integrated MSS system



As shown in Fig. 2.2, satellite eNodeB, which has similar functionality with eNodeB of CGCs, is identified in the satellite network in order to adopt terrestrial LTE radio interface to satellite specific environment while HSS and PCRF are shared for both satellite and CGC networks. Although most of entities for the integrated MSS system architecture come from those for the terrestrial 3GPP LTE network architecture, some entities should be additionally defined for common managements for the resources of the satellite and CGCs. For this, satellite/ground interworking policy server (SGIPS) is defined for interworking between the satellite and CGC as well as controlling resources of the satellite and CGC components for optimized system performance. SGIPS makes cooperation as well as information exchange between the satellite and CGCs available. In addition, SGI, which is an interface between SGIPS and MME, is defined to provide information for resource managements of the satellite and CGCs.

3 Possible deployment scenarios

3.1 Scenario 1 (frequency segmentation)

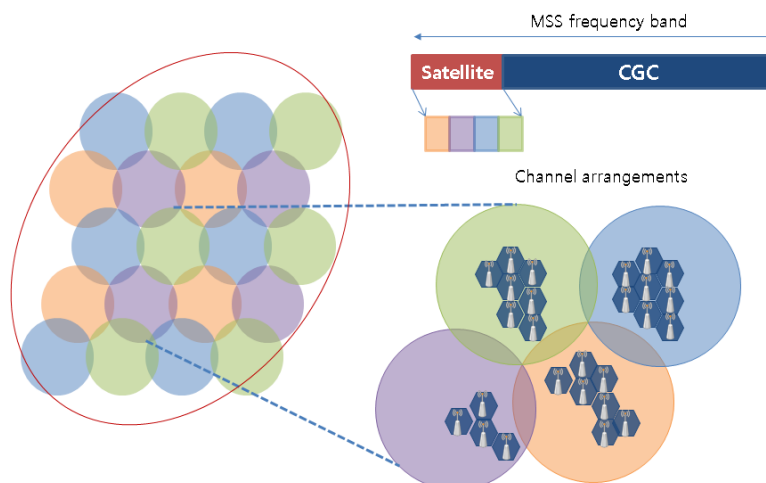
Figure 3.1 shows very simple deployment scenarios in which a satellite component and a CGC have separate frequency segments. In this scenario, several channels in the frequency segment for a satellite can be reused among multi-beams for the increase of spectral usage while the CGC is deployed with an independent frequency allocation from the satellite component.

Because the satellite component and the CGC do not suffer from co-channel interference, it is possible for them to be independently deployed without an elaborated management system. However, the use of separate frequency between them may have the following disadvantages.

- Difficulty to support satellite broadband service.
- No satellite service in the frequency segment for the CGC.

- Non-optimized usage of satellite frequency due to non-frequency reuse between the satellite component and the CGC.

FIGURE 3.1
Deployment scenario 1



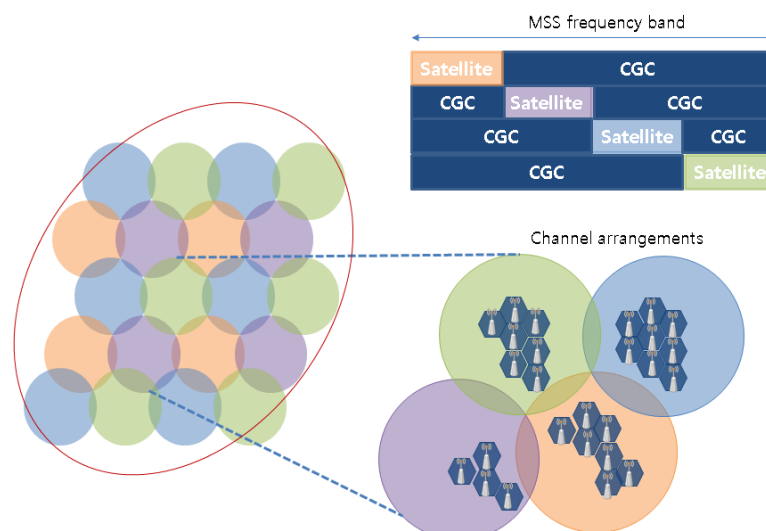
3.2 Scenario 2 (Frequency reuse)

Figure 3.2 shows deployment scenario 2 in which a satellite component and a CGC reuse satellite frequency segments together. In this scenario, several channels in the frequency segment for a satellite can not only be reused among multi-beams for the increase of spectral usage but also the CGC is deployed with reuse of the frequency segment for a satellite.

This scenario has the following advantages:

- Capability to support satellite broadband service.
- Optimized usage of satellite frequency due to frequency reuse between the satellite component and the CGC.

FIGURE 3.2
Deployment scenario 2

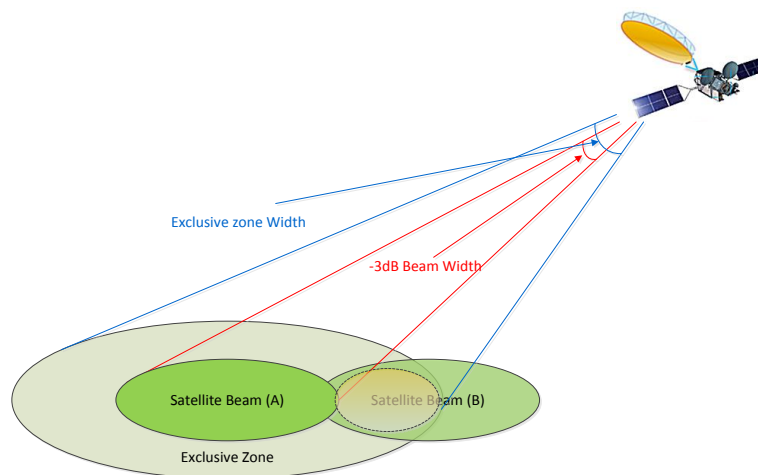


3.3 Scenario 3 (Frequency reuse with interference coordination)

Figure 3.3 shows an interference coordinated deployment scenario in which the CGC reuse satellite frequency segments under tolerable interference level to the satellite component. In this scenario, the CGC resources, which are used in the corresponding satellite beam, may be restricted to be reused in neighboring CGCs.

As seen in Fig. 3.3, to reduce intra-components interferences, the exclusive zone concept is also considered for performance evaluation. It makes restriction on reusing resources of neighboring a satellite beam by CGCs associated with neighboring satellite beam which are used for the corresponding satellite beam. Therefore, CGCs associated with a satellite beam “A” should not reuse the uplink resources of a satellite beam “B” within the area where exclusive zone is established, as well as where the satellite beam “B” covers, which belongs to neighboring satellite beam coverage as well as located at exclusive zone of the corresponding satellite beam, should not reuse the uplink resources of the corresponding satellite beam.

FIGURE 3.3
Deployment scenario 3



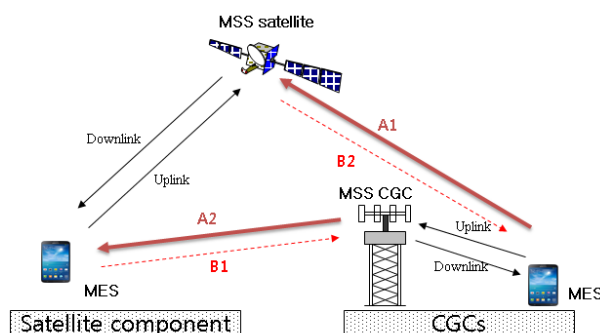
4 Performance assessment

4.1 Interference path

The following four main interference paths will be considered in an integrated MSS system as seen in Fig. 4.1.

- Path A1: from mobile earth station (MES) communication via CGCs (A) into a satellite (B) at uplink.
- Path A2: from CGCs (A) into MES communication via a satellite (B) at downlink.
- Path B1: from MES communication via a satellite (B) into CGCs (A) at uplink.
- Path B2: from a satellite (B) into MES communicating via CGCs (A) at downlink.

FIGURE 4.1
Interference paths between a satellite and a CGC



The aforementioned interference scenario is that in which both the uplink of satellite link and the uplink of CGC link share the same frequency band (vice versa for the downlinks, hereinafter, referred to as “normal mode”). An additional case would consist of the uplink of satellite link and the downlink of CGC link sharing the same frequency band (vice-versa for the downlink of satellite link and the uplink of CGC link, hereinafter, referred to as “reverse mode”). Note that in the reverse mode, interference paths differ from Fig. 4.1.

4.2 Interference assessment

Major interference problem occurs in the case of satellite uplink due to many CGC uplink signals. Therefore, only the uplink performance of the satellite component in the integrated MSS system is addressed here.

4.2.1 Propagation model

The propagation models are applied as followings:

- For the satellite component: free space path loss plus attenuation due to gaseous absorption defined Recommendation ITU-R P.676 is applied.
- For the CGCs: the modified Hata-Cost 231 median loss is applied.

4.2.2 Parameters for the satellite component

For performance assessment, the following parameters are assumed for the satellite component of an integrated MSS system. SAT-OFDM radio interface, which is included in Recommendation ITU-R M.2047 regarding the detailed specifications for the satellite radio interface of IMT-Advanced, is considered for LTE based satellite network.

TABLE 4.1

Parameters for the satellite component

The number of beam tiers	2 tier (19 satellite beams)
Frequency	2.17 GHz
Satellite height	36 000 km
Satellite Antenna pattern	Recommendation ITU-R S.672-4
Satellite antenna gain	50 dBi
3 dB beam width	0.3° (beam size of 195 km)
Frequency reuse	6 colors

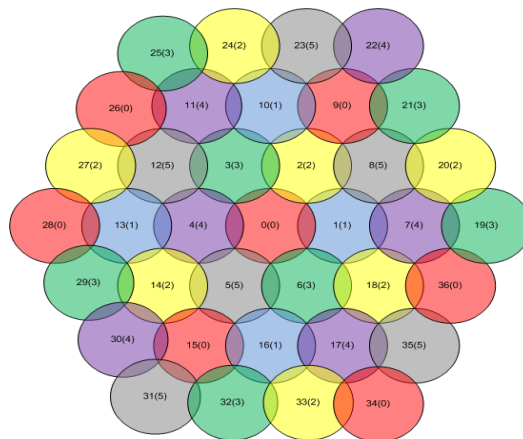
TABLE 4.1 (end)

MES per beam	25
Bandwidth per MES	180 kHz
MES Tx power (antenna gain)	Max 24 dBm, Min -30 dBm
MES antenna gain	0 dBi
Noise figure	2 dB
Shadowing from satellite MES to the satellite	Open environment in 3GPP TR 36.942

Figure 4.2 shows a satellite beam layout applying six colors frequency reuse in 2 tier beam configuration. The plan in Fig. 4.2 is configured in a way to minimize inter-beam interference. For the notation of A(B) in the figure, A and B represent the satellite beam number and the satellite carrier number (one of 6 satellite carriers), respectively.

FIGURE 4.2

Satellite beam configuration



4.2.3 Parameters for the CGCs

For performance assessment, the following parameters are assumed for the CGCs of an integrated MSS system. LTE radio interface, which is included in Recommendation ITU-R M.2012 regarding the detailed specifications for the terrestrial radio interface of IMT-Advanced, is considered for LTE based CGC network.

TABLE 4.2

Parameters for the CGC

Cell radius	1 km
Frequency reuse	1 color (3 sector)
CGC Tx power	43 dBm
Antenna pattern	3GPP TR 36.942
CGC antenna gain	15 dBi
Frequency	2.17 GHz
MES Tx power (antenna gain)	Max 250 mW, Min -30 dBm

TABLE 4.2 (*end*)

MES antenna gain	0 dBi
Outdoor wall penetration loss	10 dB
Uplink power control	Applied
Shadowing from CGC MES to the satellite	Urban environment in 3GPP TR 36.942

The CGCs can reuse satellite frequencies which are not only used by adjacent satellite beams but also have no consideration for the satellite beam in the area where the CCCs are deployed.

Uplink power control is based on the following equation:

$$P_{tx} = \min(P_{max}, P_o + 10\log(N) + \alpha \cdot PL)$$

where P_{max} , PL , and N denote the max MES transmit power, path loss, and the number of assigned resource blocks (RBs).

TABLE 4.3

Parameters for the uplink power control in CGCs

Parameter set	Alpha	P_o PUSCH(i) [dBm]	
		40 MHz (LTE-A)	10 MHz (LTE)
Set 1	1	-101	-101
Set 2	0.8	-92.2	-92.2

4.2.4 Interference assessments

4.2.4.1 Interference analysis in deployment scenario 2

In an integrated MSS system, severe interference from a lot of MES communicating via CGCs into a satellite are existed for uplink.

Figure 4.3 represents the transmit power distribution for the MES communicating via CGCs when a power control scheme is applied. Resource block (RB) of LTE in Fig. 4.3 corresponds to 180 kHz. From the Figure, it is noted that average uplink transmit power for the CGC MES is about 7.9 dBm/180 kHz.

FIGURE 4.3
Uplink power distribution for the MES communicating via CGC

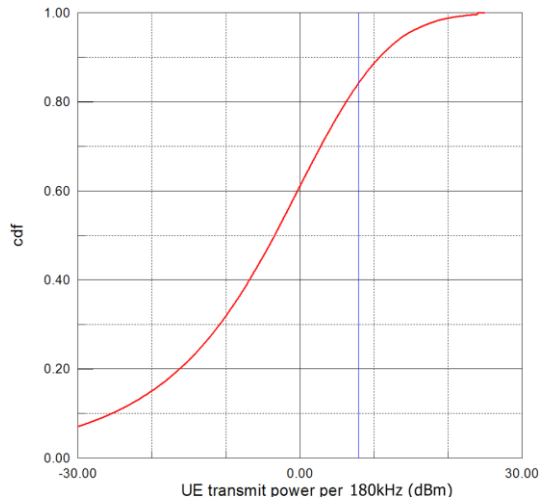
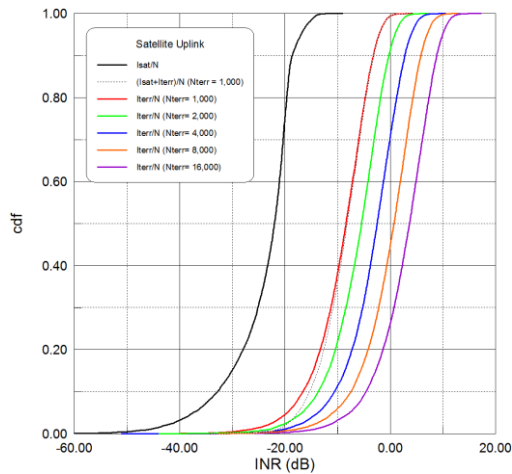


Figure 4.4 represents the uplink interference from the CGC MES into the satellite. The CGC MES is uniformly distributed over the satellite beams except the satellite beams with the satellite carrier number #0 in Fig. 4.2 and then, the uplink interference is measured in the beam number #0. From Fig. 4.4, it is noted that the uplink interference from the CGC MES into the satellite is considerably severe and the interference level is increased twice as the number of the CGC MES (denoted as N_{terr} in Fig. 4.4) is increased twice.

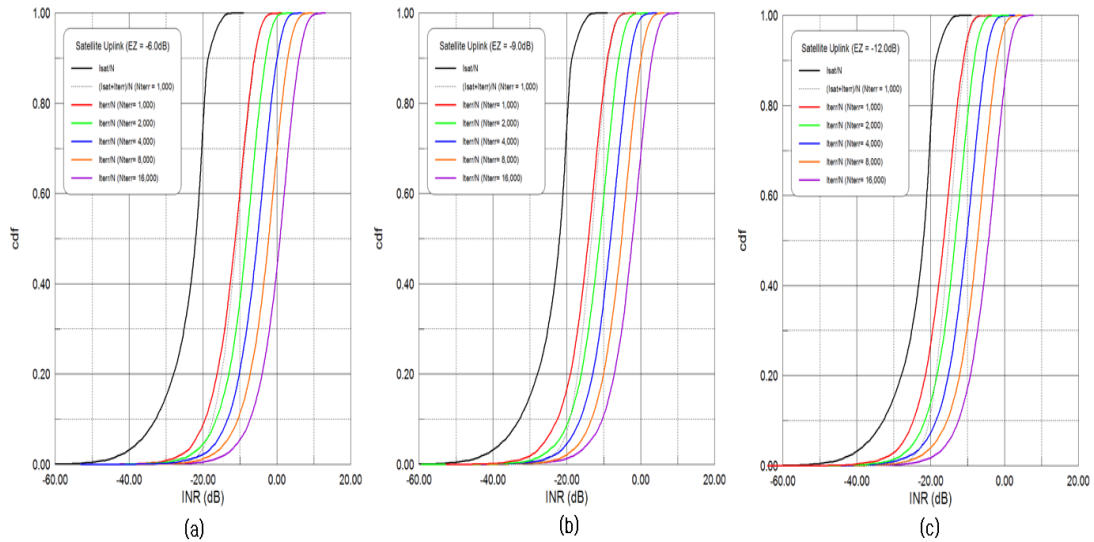
FIGURE 4.4
Cumulative distribution function of I/N vs the number of the CGC MES



4.2.4.2 Interference analysis in deployment scenario 3

Figure 4.5 shows the uplink interference from the CGC MES into the satellite according to exclusive zone levels, -6 dB, -9 dB and -12 dB. Similar to Fig. 4.4, the interference level is increased as the number of the CGC MES is grown up while exclusive zone makes the interference level appropriately decreased. It is noted in the Figure that the interference level is maintained if the exclusive zone level is decreased as -3 dB when the number of the CGC MES (denoted as N_{terr} in Fig. 4.4) is increased as 3 dB.

FIGURE 4.5
Cumulative distribution function of I/N vs according to exclusive zone

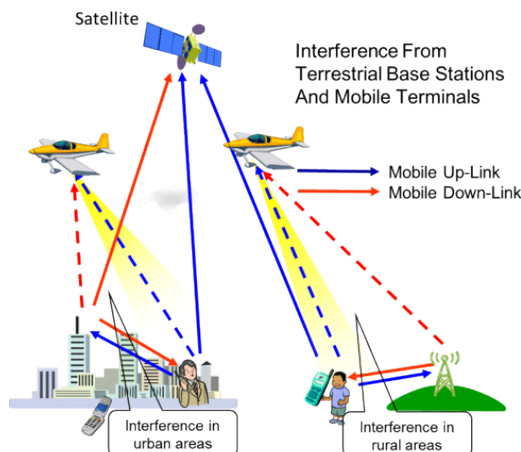


4.2.4.3 Other possible interference analysis for deployment scenario 3

In the integrated MSS system, the mobile terminal has a seamless connection to both the CGC and satellite components with these CGC and satellite components sharing the same frequency band under the co-channel interference. In this study, the system capacity of CGC and satellite components under co-channel interference was evaluated to verify frequency sharing between CGC and satellite components. The system capacity was evaluated using power transmission measurements from existing wideband code division multiple access (W-CDMA) cellular phones and base stations as reference data.

As shown in Fig. 4.2, a major interference problem can occur during satellite uplink due to multiple CGC uplink signals. Because of this, only the uplink performance of the satellite component and CGC in the integrated MSS system is addressed here. To assess the performance of the two possible interference scenarios (normal mode and reverse mode), a measurement campaign was conducted to evaluate the radiation power of existing mobile base stations and cellular phone terminals during transmission using an airplane as shown in Fig. 4.6.

FIGURE 4.6
Schematic of measurement campaign using airplane

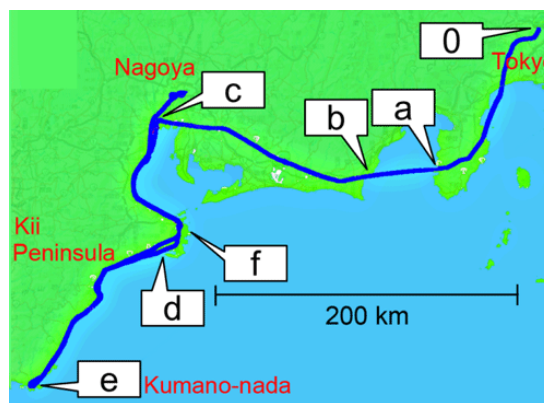


Due to the variation of the density of mobile base stations and terminals in Japan, the measurement campaigns were carried out in several areas as shown in Fig. 4.7, including suburbs and urban areas. Here, the urban area is assumed to have 10 IMT base stations per square km, while the suburban regions have one or two base stations per square km. The experimental methodology is outlined below.

The places of the measurement are as follows:

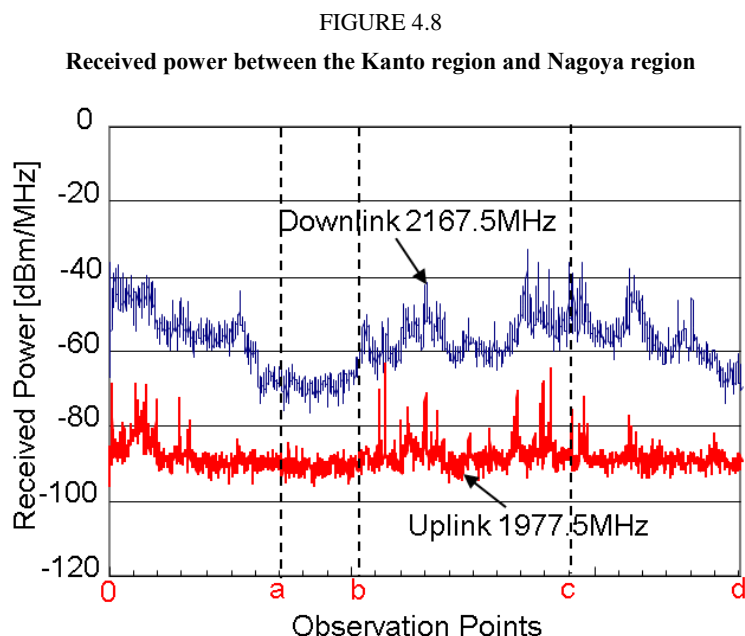
- Rural and urban areas around Tokyo and off the coast of Choshi.
- Long distance route over 500 km between the Kanto region and the Kii peninsula.
- Thinly populated areas with population density of 100 or less per square km.

FIGURE 4.7
Schematic of experiment using aircraft



In order to estimate the amount of radiation from Japan, we collected data from the Kanto region to Nagoya and the Eastern Kii Peninsula, as shown in Fig. 4.7. Along this segment, we were able to collect data from a high population density region (the Kanto Plain), from low population density regions (Izu Peninsula, coast of Enshu, Mikawa Bay), and over the sea (Suruga Bay). This measurement data is expected to enhance the accuracy of radiation estimates in Japan.

An example of the received power measured between the Kanto region and Nagoya region is shown in Fig. 4.8. It is observed that the uplink channel reception strength is approximately 25 to 30 dB less than that for the downlinks channel and that several peaks are detected over the urban area, marked as 'c'. It is thought that these peaks occur as a result of passing above base stations.



It is clear that the received power varies as a function of the measurement region and that the received power in the downlink channel is larger than the uplink channel by 25~30 dB. This result shows that the use of normal mode may reduce the interference to the satellite. Because of this, system capacity analysis was performed using the normal mode scenario.

4.2.4.3.1 Parameters for the satellite component

Satellite component link parameters for a case of GSO are listed in Table 4.4 and satellite beam allocation is shown in Fig. 4.9 with an estimated 83 satellite beams covering Japan and the exclusive economic zone (EEZ). A 4.3 MHz sub-band is assigned to each satellite beam (seven beam = one cluster = 30 MHz) and the transmission power of each satellite link is 200 mW. The maximum number of satellite links, 10 000, is derived from the estimated total transmission power of each satellite, 2 kW. In the normal period, terminals are assumed to be uniformly distributed while during a disaster period, the maximum number of satellite channels which are able to be assigned to one satellite beam are assumed to be in use. This is realized by changing the frequency band allocation for each satellite beam using the channelizing function of satellite transponder.

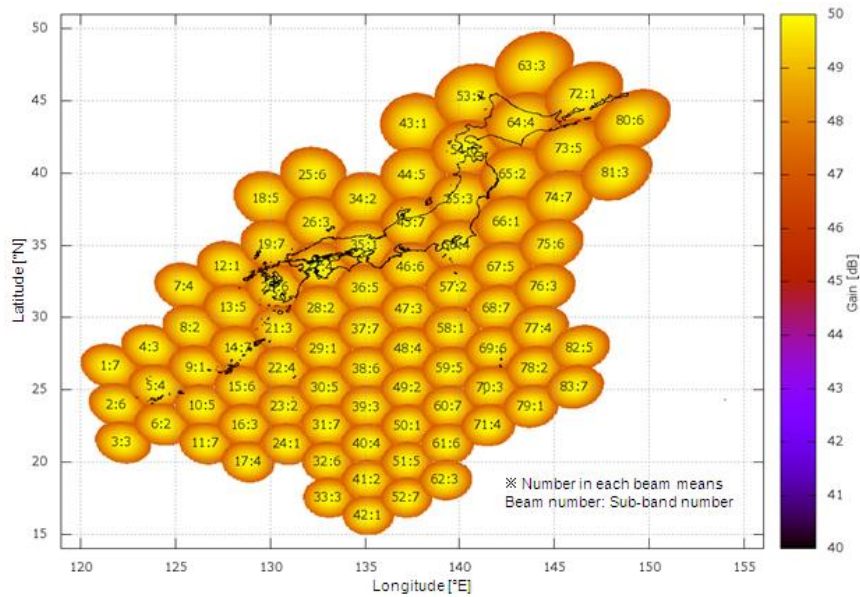
TABLE 4.4

Link parameters for satellite component

Items	Link parameters
Satellite orbital position	136°E (GSO)
Access scheme	FDMA
Uplink frequency (MHz)	1980-2010
Downlink frequency (MHz)	2170-2200
Number of sub-band	7
Sub-band bandwidth (MHz)	4.3
Information rate (kbps)	9.6
Occupied bandwidth/channel (kHz)	19.2
Satellite antenna diameter (m)	30
Minimum gain in satellite cell (dBi)	47
Satellite antenna pattern	Rec. ITU-R S.672-4
Satellite antenna sidelobe level (dBi)	30
Satellite total trasmit power (kW)	2
Satellite transmit power/channel (mW)	200
Satellite required C/N0(dB-Hz)	43.8
Satellite antenna noise temperature (K)	300
Satellite feeder loss (dB)	1.1
Satellite noise figure (dB)	1.5
Terminal antenna gain (dBi)	0
Terminal transmit power (mw)	200
Terminal required C/N0 (dB-Hz)	43.8
Terminal antenna noise temperature (K)	80
Terminal feeder loss (dB)	1
Terminal noise figure (dB)	1.5

FIGURE 4.9

Satellite beam allocation



4.2.4.3.2 Parameters for the CGC

CGC link parameters are listed in Table 4.5. In the CGC link, the service area is divided into many grids (grid size = around 10 km). The number of terminals and base stations, and their transmission power within each grid is determined. The number and transmission power of base stations are determined using radio station license information in Japan from 2010. The number of terminals is calculated using the daytime population for each grid and assumed call rate (1%). The transmission power of terminals for each population class is estimated based on a statistical analysis of W-CDMA cellular phone transmission power measurement data obtained during the measurement campaign in Japan. This is applied as the transmission power of terminal. A block diagram of the measurement system is presented in Fig. 4.10 showing that the cellular phone output power is measured using a power meter. Three common 3G cell phone carriers were available in Japan at this time and the measurement frequency was primarily in the 2 GHz band. Realistic measurement conditions (i.e. Phantom) were available and the position of the test van was recorded using navigation software and GPS. The experimental field image was recorded in digital video recorder. Figure 4.11 shows the average output power vs. population density. Low output power, less than -5 dBm, was observed in dense urban and urban areas while maximum power, 7 dBm, was observed in rural areas. Importantly, these measured powers were much lower than the maximum capability of W-CDMA cellular phone of $+24$ dBm. These results indicate that the average output power decreases as population density increases for both carrier “X” and “Y”.

TABLE 4.5

Link parameters for the CGC link

Items	Link parameters
Access scheme	CDMA
Uplink frequency (MHz)	1980–2010
Downlink frequency (MHz)	2170–2200
Number of sub-band	6
Sub-band bandwidth (MHz)	5
Information rate (kbps)	9.6
Occupied bandwidth/channel (kHz)	5000
Antenna gain of BS at satellite direction (dBi)	-3
Antenna gain of BS at terrestrial direction(dBi)	17
Transmit power for BS	30% of transmit power of radio station license information for cellular phone base station in Japan
BS required C/N0 (dB-Hz)	47.6
BS antenna noise temperature (K)	200
BS feeder loss (dB)	0
BS noise figure (dB)	1.5
Terminal antenna gain (dBi)	0
Terminal transmit power	Estimated by statistical analysis of measured data of W-CDMA cellular phone transmit power obtained by measurement campaign in Japan (below 1mW)
Terminal required C/N0 (dB-Hz)	47.6
Terminal antenna noise temperature (K)	80
Terminal feeder loss (dB)	0
Terminal noise figure (dB)	1.5

FIGURE 4.10

Block diagram of measurement system for cellular phone transmission power

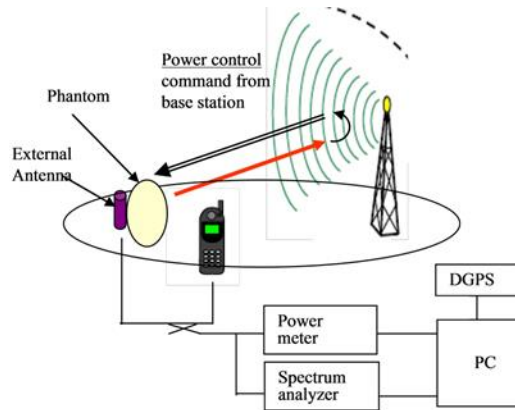
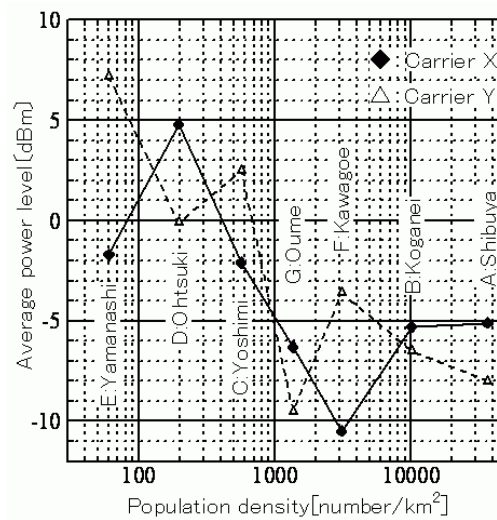


FIGURE 4.11

Transmission power of cellular phone vs. population density



As shown in the transmission power measurement results, the average transmission power of the cellular phone was less than 1 mW, much lower than the maximum cellular phone transmission power of approximately 250 mW.

4.2.4.3.3 Capacity analysis under co-channel interference

A capacity evaluation was performed for the cases in which only the (a) interference caused by CGC link was considered (interference caused by satellite link is ignored), (b) interference caused by satellite link was considered (interference caused by CGC link is ignored), and (c) both interferences caused by satellite and CGC links were considered. The calculation procedure is described as follows. By using an interference calculation simulator, received signal power and interference signal power are calculated for each interfered link. Obtained values are then used to calculate the capacity using the following procedure.

- a) Average interference level for each link is calculated based on the equation

$$\bar{I} = \frac{\sum_{m=1}^M I_m \cdot B}{M} \quad (1)$$

where M is number of interfering links in which the frequency band overlaps with the interfered link, I_m is the interference level for m -th interfering link, and B is the ratio of frequency band overlap between m -th interfering link and interfered link.

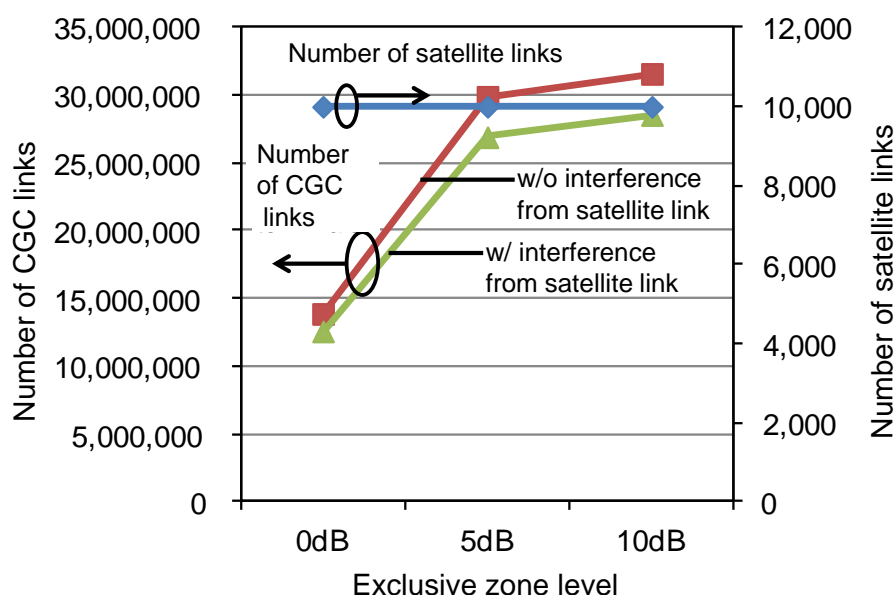
- b) Link coefficient a , the maximum number of interfering links under the condition that particular interfered link satisfies required C/N_0 , is calculated based on the following equation

$$\frac{C}{(a \cdot \bar{I} + N_0)} = \left[\frac{C}{N_0} \right]_{req} \quad (2)$$

The effect of the exclusive zone is also evaluated by setting exclusive zone levels at 0 dB, 5 dB and 10 dB.

Satellite uplink suffers from the interference caused by CGC uplinks using the same sub-band outside the satellite cell, and from the interference caused by satellite uplink using the same sub-band in other satellite cells. The result of the capacity calculations are shown in Fig. 4.12. The number of satellite links is 10,000, which means that the satellite link is established independent on the level of exclusive zone. When the exclusive zone level is 0 dB, the number of CGC links without interference from satellite link is 14 million and that with the interference from satellite link is 13 million. The maximum number of links is observed when the exclusive zone level is 10 dB. On the other hand, the communication area for CGC link is 100%, 88% and 31% when the exclusive zone level is 0 dB, 5 dB and 10 dB, respectively. This indicates that the communication area for CGC links decreases as the exclusive zone level increases.

FIGURE 4.12
CGC and satellite uplink capacity under co-channel interference



4.3 Throughput assessment

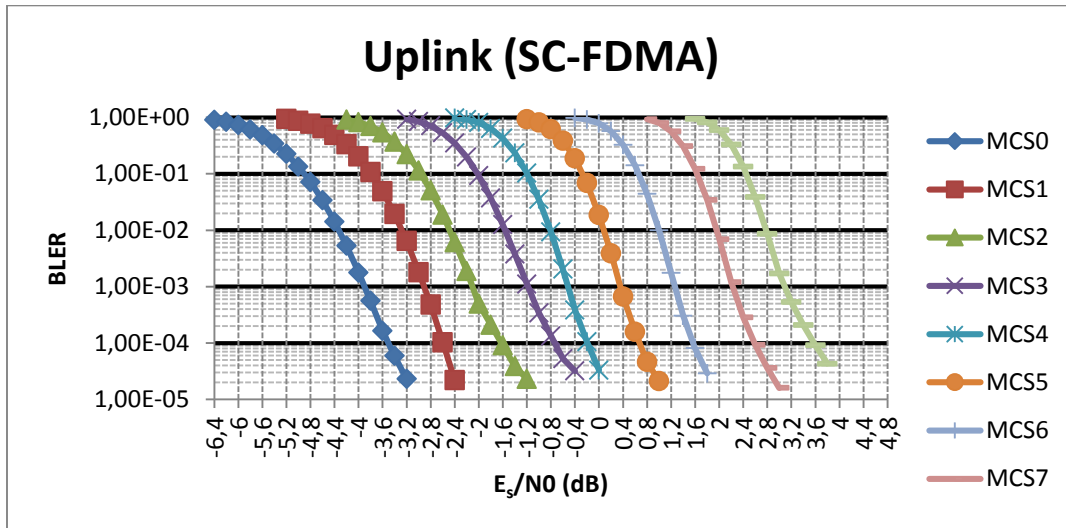
4.3.1 Link performance and impact on SINR

In the same context with interference assessment, major signal to interference plus noise ratio (SINR) degradations occurs in the case of satellite uplink due to many CGC uplink signals.

Therefore, only the uplink performance of the satellite component in the integrated MSS system is addressed here.

Figure 4.13 shows the uplink performance of SAT-OFDM radio interface according to various modulation and coding scheme (MCS) modes.

FIGURE 4.13
Uplink performance of the satellite component



From Fig. 4.13, the required SINRs for each MCS mode for block error rate (BLER) of 10^{-2} are listed up in Table 4.6.

TABLE 4.6
Required SINR for MCS in the satellite component

MCS mode	Data rate	Required SINR for BLER of 10^{-2}
0	16 kbit/s	-4.3 dB
1	24 kbit/s	-3.3 dB
2	32 kbit/s	-2.5 dB
3	40 kbit/s	-1.5 dB
4	56 kbit/s	-0.8 dB
5	72 kbit/s	0.1 dB
6	88 kbit/s	1.0 dB
7	102 kbit/s	2.0 dB
8	120 kbit/s	2.8 dB

Figures 4.14, 4.15 and 4.16 show the SINR degradation of satellite uplink according to the number of CGCs in cases of no application of exclusive zone and application of exclusive zone of -6 and -12 dB, respectively. NCGC represents the number of CGCs.

FIGURE 4.14

SINR degradation of the satellite component

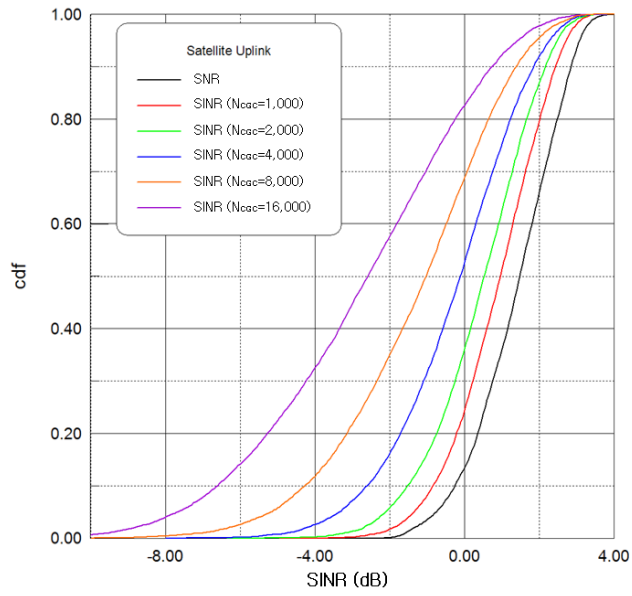


FIGURE 4.15

SINR degradation of the satellite component (exclusive zone of -6 dB)

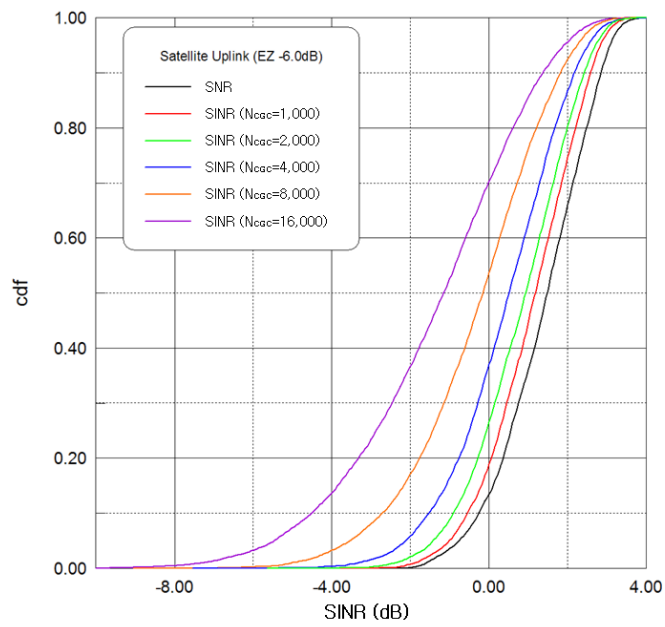
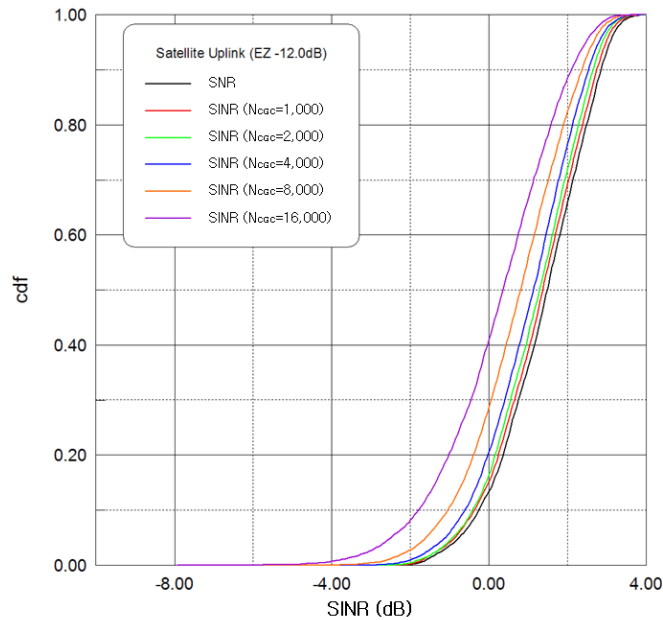


FIGURE 4.16

SINR degradation of the satellite component (exclusive zone of -12 dB)

As shown in the Figures above, as the number of CGC increases, SINR degradation of satellite component gets worse. However, with application of exclusive zone for CGC, SINR degradation of satellite component can be improved.

4.3.2 Satellite resource availability in CGCs

The allowable number of CGCs and the averaged MES transmit power could be determined according to the supported MCS mode in the uplink of SAT-OFDM. For example, when the MES of the satellite component needs services with BLER of 10^{-2} corresponding to only MCS mode 0, the satellite uplink requires SINR of more than -4.3 dB, assuming the availability of 99%. Therefore, aggregated total transmit power per RB from CGCs, which is calculated by the number of CGCs and their MES transmit power per RB, should be limited to 42.9 dBm. It means that one thousand CGCs holding the MESs with average transmit power per RB, 12.9 dBm are allowable and, in the case, when one thousand CGCs are deployed in the integrated MSS system, satellite resource availability would be maximized with satisfying the service requirement of satellite component.

Tables 4.7 to 4.11 show LTE RB availability in CGCs of the integrated MSS systems, assuming that the UE of the satellite component needs services with BLER of 10^{-2} corresponding to only MCS mode 0. They represent the cases for no satellite frequency reuse in CGCs, the UE transmit power per RB of 0 dBm and no exclusive zone, the UE transmit power per RB of 6 dBm and no exclusive zone, the UE transmit power per RB of 0 dBm and the exclusive zone of -9 dB, and the UE transmit power per RB of 6 dBm and the exclusive zone of -9 dB, respectively.

TABLE 4.7

LTE RB availability in CGCs (no satellite frequency reuse)

Satellite bandwidth per beam	CGC bandwidth per cell	Satellite RB	CGC RB	Satellite RB availability	CGC RB availability
5 MHz	0 MHz	25	0	25	0
3 MHz	12 MHz	15	60	15	60
1.4 MHz	21.4 MHz	6	106	6	106

TABLE 4.8

LTE RB availability in CGCs (CGC Tx power/RB: 0 dB, no exclusive zone)

Satellite bandwidth per beam	CGC bandwidth per cell	Satellite RB	CGC RB	Satellite RB availability	CGC RB availability
5 MHz	0 MHz	25	0	25	0
3 MHz	12 MHz	15	60	15	60
1.4 MHz	21.4 MHz	6	106	6	106

TABLE 4.9

LTE RB availability in CGCs (CGC Tx power/RB: 6 dB, no exclusive zone)

Satellite bandwidth per beam	CGC bandwidth per cell	Satellite RB	CGC RB	Satellite RB availability	CGC RB availability
5 MHz	25 MHz	25	125	25	4.0
3 MHz	26 MHz	15	130	15	62.2
1.4 MHz	28 MHz	6	140	6	107.1

TABLE 4.10

LTE RB availability in CGCs (CGC Tx power/RB: 0 dB, exclusive zone: -9 dB)

Satellite bandwidth per beam	CGC bandwidth per cell	Satellite RB	CGC RB	Satellite RB availability	CGC RB availability
5 MHz	25 MHz	25	125	25	63.6
3 MHz	26 MHz	15	130	15	95.6
1.4 MHz	28 MHz	6	140	6	123.3

TABLE 4.11

LTE RB availability in CGCs (CGC Tx power/RB: 6 dB, exclusive zone: -9 dB)

Satellite bandwidth per beam	CGC bandwidth per cell	Satellite RB	CGC RB	Satellite RB availability	CGC RB availability
5 MHz	25 MHz	25	125	25	16.0
3 MHz	26 MHz	15	130	15	69.0
1.4 MHz	28 MHz	6	140	6	110.3

From the above evaluation results, it is noted that the satellite frequency reuse in the CGCs of the integrated MSS system increases satellite spectrum utilization as well as the CGC deployment in indoor and urban environments have benefits to increase the number of allowable CGCs, compared to that of CGCs in rural and suburban environment. In addition, for system performance enhancement, intelligent resource management schemes such as the exclusive zone concept need to be applied together.

4.3.3 Throughput degradation in the satellite components

4.3.3.1 Simulation parameters

Effect of the interference from the CGC network on throughput performance in the satellite components can be assessed via system-level simulation.

In the system-level simulation for performance assessment in the satellite components, the following parameters in Table 4.12 are considered.

TABLE 4.12

System-level simulation parameters

General parameter	
The number of beams	19 (2 tier)
Distance between beam centre	180 km
The number of MESs per beam	25
MESs distribution	Random
Downlink carrier frequency	2.1 GHz
Uplink carrier frequency	2.0 GHz
Bandwidth per beam	5 MHz
Frequency reuse factor	6
Modulation and coding scheme (MCS) modes	From MCS0 to MCS16
Target BLER of MCS mode	10^{-2}
Backoff for AMC mode decision	2 dB
The number of Stop and Wait HARQ processes	500
Maximum number of HARQ retransmission	3

TABLE 4.12 (*end*)

General parameter	
ARQ transmission window size	1500 PDUs
Maximum number of ARQ retransmission	2
Channel environment	Open, suburban, urban
Scheduling method	Proportional fairness
Power control	Full power allocation
Traffic model	Full buffer
Link-to-system mapping	Effective exponential SINR mapping
Satellite parameter	
Antenna heights	36 000 km
Number of transmit antenna	1
Number of receive antenna	1
Antenna radiation pattern	Recommendation ITU-R S.672-4
Antenna gain	50 dBi
Power for communication payload	3.8 kW (200W per beam)
Loss of nonlinearity	3 dB
Other loss	1.5 dB
System noise temperature	450°K
User terminal parameter	
Antenna heights	1.5 m
The number of transmit antenna	1
The number of receive antenna	1
Antenna radiation pattern	Omnidirectional
Antenna gain	0 dBi
MES transmit power	250 mW, 2W
Other loss	3 dB
System noise temperature	290°K

4.3.3.2 Performance in open environments

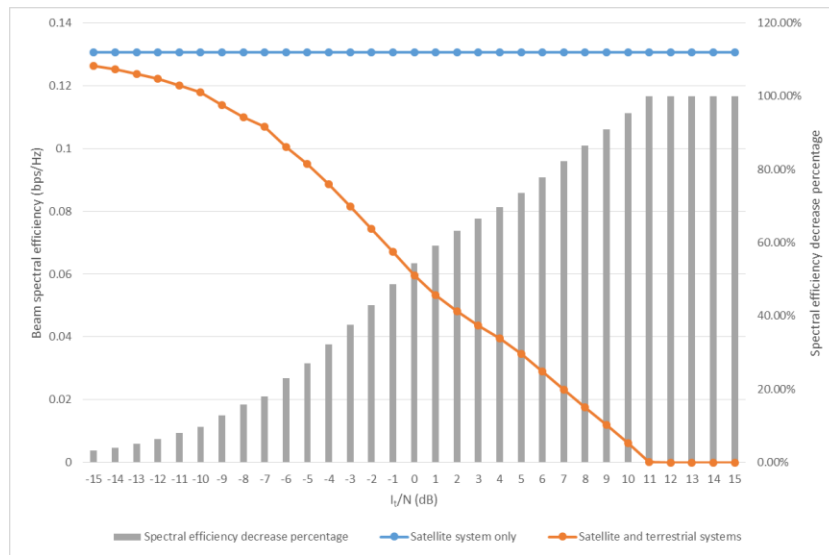
4.3.3.2.1 Uplink performance

Figure 4.17 shows average uplink spectral efficiency in the satellite component according to the interference level from the MES communicating via CGCs.

As seen in the Figure, because the satellite MES with maximum transmit power of 250 mW secures not enough link margin, performance degradation is very sensitive to the interference from the CGC MESs. For example, when I/N value is assumed to -10 dB and 0 dB, performance degradation of 9.7% and 54.4% are shown in the satellite uplink, respectively.

FIGURE 4.17

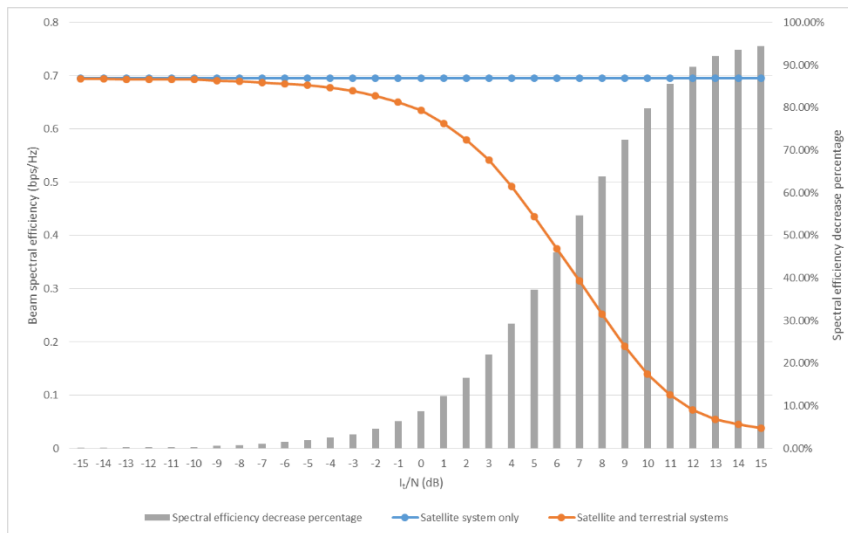
Uplink performance for the satellite component (250 mW MES) in open environments



On the other hands, Fig. 4.18 shows average uplink spectral efficiency for the MES with maximum transmit power of 2 W in the satellite component. As seen in the Figure, because the satellite MES with maximum transmit power of 2 W secures some link margin, performance degradation is less sensitive to the interference from the CGC MESs than that in case of 250 mW MES.

FIGURE 4.18

Uplink performance for the satellite component (2 W MES) in open environments



It is noted in Fig. 4.18 that when I/N value is assumed to -10 dB and 0 dB, performance degradation of 0.35% and 8.59% are shown in the satellite uplink, respectively.

5 Technical constraints associated with deployments

5.1 Large antenna and multi-beam technology

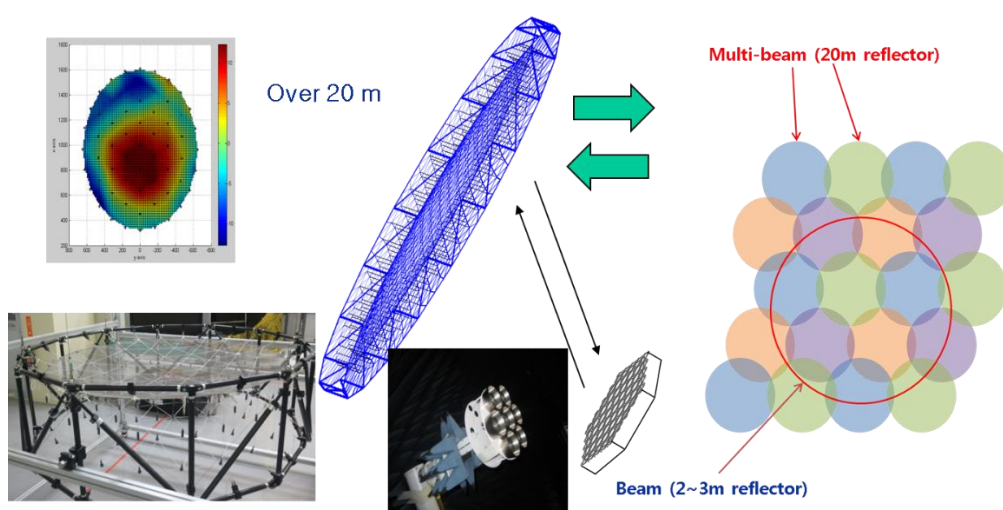
For the efficient use of satellite frequency, MSS systems have evolved to introduce multi-beam satellites with large number of beams (up to few hundreds). A satellite antenna with large size of

reflector allows a number of small spot-beams to be formed. It enables using satellite frequency reuse with high reuse factors, and thus system capacity to be increased. In addition, the large satellite antenna will make possible reuse of terrestrial terminal with small form factor without any extra equipment due to high antenna gain. It will definitely help in the realization of low-cost low-size single-mode UE encompassing both terrestrial and satellite components. Figure 5.1 shows multi-beam technology with large antenna.

When the satellite with 20 m size of reflector is applied, we can make many multi-beams over European coverage and the satellite frequency can be highly reused for the increased system capacity. In North America, Terrestrial has already launched this kind of large antenna, Terrestrial-1 in order to provide coverage to the North America. Terrestrial-1 offers approximately 500 dynamically configurable spot beams allowing Terrestrial to allocate spectrum and capacity based on ground based beam forming (GBBF) which is addressed in the next clause.

FIGURE 5.1

Multi-beam technology with large antenna (example)



5.2 Radio interface techniques

A new satellite radio interface (SRI) technology to provide broadband services could be introduced. Maximizing the commonality between satellite and CGC radio interfaces is one of the most important factors for cost-effective service delivery as well as the implementation of common cost-effective user terminal by possibly reusing CGC UE. Table 5.1 lists up considerable satellite radio interfaces for the satellite component of an integrated MSS system.

TABLE 5.1

Considerable radio interfaces

Satellite radio interfaces	Terrestrial radio interfaces
GMR-1	GSM
EGAL	CDMA-2000
SAT-CDMA	WCDMA
SAT-OFDM	LTE

GMR-1 radio interface has already been adopted for Thuraya and Terrestar satellite systems and supports narrowband services up to a few hundreds of kbit/s data rates. EGAL radio interface was developed by Qualcomm and incorporated into a multi-functional chip of Qualcomm as seen in Fig. 5.2. For possible implementation of cost-effective integrated terminal, most SRIs for MSS are based on terrestrial radio interface for MS. Figure 5.2 shows a Terrestar's Blackberry type terminal with similar cost of existing terrestrial terminal (\$ 799). Only satellite RF module is added into existing terrestrial terminal with no severe cost increase and no extra antenna. Of course, with extra antenna, more broadband service could be supported (e.g. additional cost of \$ 300 in case of Terrestar).



5.3 Interworking between the satellite and CGCs

In those integrated MSS systems, one of key issues is how to optimize the spectral efficiency of the MSS system as a whole (satellite plus CGC) in terms of severe interference problems and asymmetric traffic demands between a satellite and CGCs as well as how to make seamless connectivity between two components.

In that sense, common resource and network management between the satellite and CGCs should be carefully considered. The frequency reuse between satellite and CGCs will inevitably imply co-channel interferences that might cause performance degradation of the MSS system. Therefore, intelligent interworking and common resource management scheme may inevitably need to be incorporated in an integrated system. However, common control of the satellite and CGCs network may impose huge burden in satellite gateway due to high complexity.

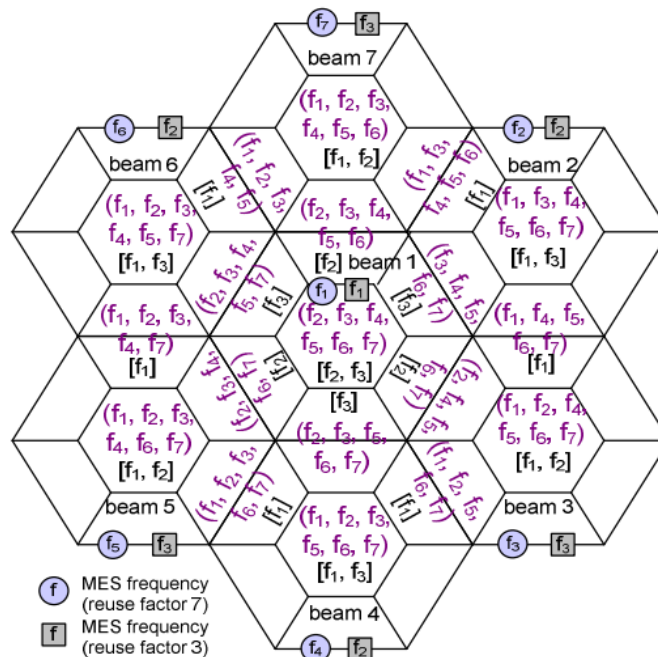
6 Technical enablers for performance enhancements

6.1 Efficient frequency reuse schemes

As mentioned before, the frequency reuse between satellite and CGCs will inevitably imply co-channel interferences that might cause performance degradation of the MSS system. Therefore, the precise frequency reuse plan in both the satellite and CGCs is very important in an integrated MSS system, and thus makes satellite frequency utilization increased.

For example, Fig. 6.1 represents a frequency reuse scenarios with reuse factors, 7 and 3. Multi-beam satellite communicates with MES using frequency from f_1 to f^7 (reuse factor 7) and from f_1 to f_3 (reuse factor 3) in each satellite beam. Each beam is sectioned into seven regions and all the available reuse frequencies are divided in each beam. The CGCs use the frequency which is not allocated for MES. Frequency group in satellite beam means the reused frequency in CGCs.

FIGURE 6.1
Frequency reuse pattern for an integrated MSS system



It is noted that the CGC MES can reuse satellite resources when only one of the seven frequencies is allocated for the satellite MES. When the satellite MES is in area of beam 1, the CGC MES at the centre of beam 1 can reuse the satellite resources of the frequencies from f_2 to f_7 with negligible intra-beam interference to the satellite MES. The CGC MES at the edge of beam 1 can induce the interference to the satellite MES in adjacent beam. The CGC MES at the centre of each beam reuses frequencies except the allocated frequencies for the satellite MES in the targeted edge, while the CGC MES at the edge of each beam reuses the frequencies except the frequencies in the targeted and adjacent beam edges.

As another example, exclusive zone in addressed in sub-clause 4.2 could also be considered for one of efficient frequency reuse schemes.

6.2 Interference management schemes

In addition to efficient frequency reuse techniques, intelligent resource allocations and interference management techniques can be also considered for performance enhancement of an integrated MSS system by reducing interference between satellite and CGCs.

For example, Fig. 6.2 shows inter-component interference between the satellite beam and CGC cells. Since inter-component interference can degrade the performance, it is essential to limit it. It is expected to mitigate the inter-component interference within the integrated MSS system by minimizing the required power to serve all beams and CGC cells with different traffic demands under bandwidth constraints as seen in Fig. 6.3. The constraint is imposed in order to prevent extreme interference by allocating the same amount of bandwidth to whole beams and CGC cells operating at the same frequency, f_i . From some optimization techniques, it is noted that this kind of dynamic resource management can not only achieve less inter-component interference by saving the total transmit power to serve the required data rates compared to a uniform resource allocation but also obtain better capacity gain.

FIGURE 6.2

Inter-component interference between satellite beams and CGC cells

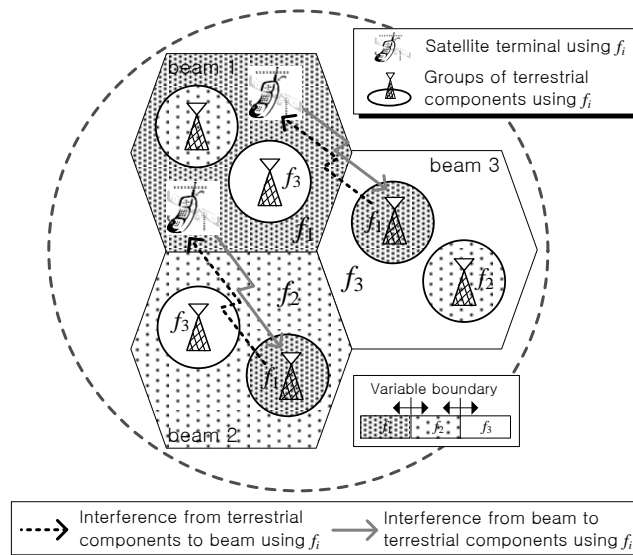
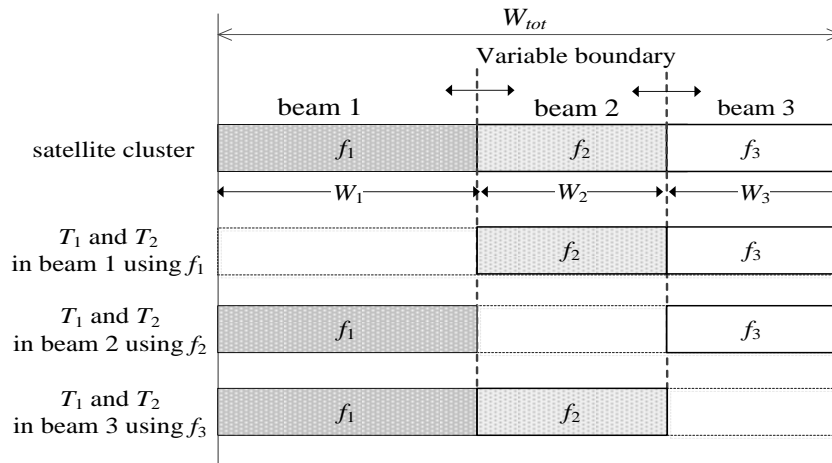


FIGURE 6.3

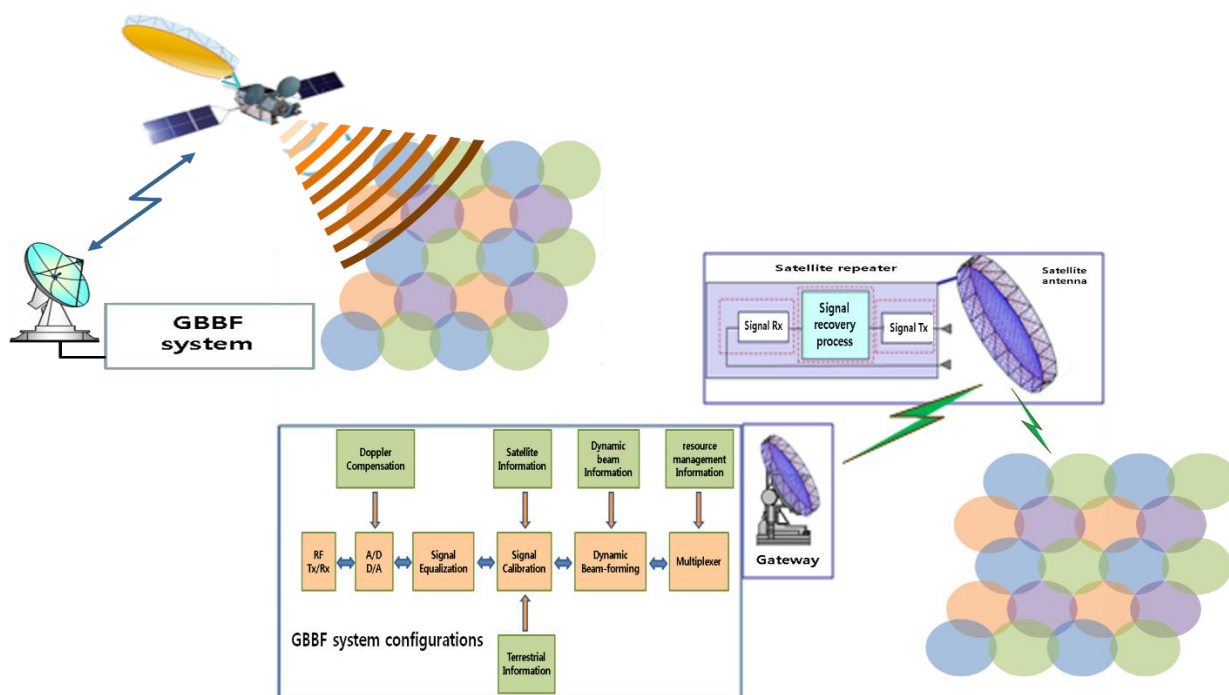
Bandwidth constraints for minimization of inter-component interference



6.3 Ground based beam-forming schemes

Figure 6.4 shows the structure of ground based beam-forming (GBBF) to implement an intelligent integrated MSS system. The GBBF can be adopted to deliver unprecedented flexibility to provide broadband services through stable and configurable beams. In addition, it allows transparent satellite to be used regardless of applied satellite radio interface technologies as well as huge signal processing for interference mitigation to be mounted in ground.

FIGURE 6.4
GBBF system concepts



Because GBBF techniques enables a low cost bent-pipe satellite based MSS system, it can be exploited in satellite payloads to allow adapting to new satellite transmission waveform in the future.

6.4 Satellite based digital beam-forming and channelizing schemes

Current performance improvements of application specific integrated circuit (ASIC) and field-programmable gate array (FPGA) will enable digital onboard processors to become a reality. Recently, hundred-class multi-beam forming has been realized by on-board digital beam former (DBF) technology. The digital channelizer switches and arranges channels in the feeder-link bandwidth, enabling improvements in the spectrum efficiency of the feeder-link bandwidth, and flexible resource re-allocation depending on the spatial/temporal change of traffic demand. These technologies are applicable to integrated MSS system satellites that are required to maintain number of spot beam and enhance system performance.

Current MSS systems employing onboard DBF/channelizer have been realized by Thuraya and Immarsat. Thuraya has 246 multi beams and function of resource control (resource control unit: 156.25 kHz).

As an example, a small-scale DBF/channelizer developed for ground validation is presented in the Attachment.

Attachment

Development of small-scale prototype DBF/channelizer as an example of technical enablers

1 Introduction

An example of an integrated MSS system covers the required service area by using 30 m-class-diameter large satellite antenna, in which around hundred multi-beam systems are required. The sidelobe level of the satellite antenna needs to be maintained at a low level to suppress the beam-to-beam interference level in multibeam system, and to suppress the interference level to/from other systems. While analog beamforming may not be practical for satisfying these requirements, onboard digital beamforming could be advantageous due to its scalability and flexibility. Generally, satellite and terrestrial traffic is continuously changing and asymmetrically distributed over a wide area. Especially in an emergency situation such as a disaster, traffic is primarily distributed in the disaster areas. Therefore satellite resources (i.e. frequency and power) need to be allocated to each satellite beam depending on the traffic state. Because of its flexibility, on-board digital channelizing is a potential technological solution for satisfying this need.

Regarding these requirements for satellite onboard communications system, studies on the satellite onboard technologies such as the multi beamforming, low sidelobe, and reconstruction of resource allocation have been conducted and are detailed below.

Figure A.1 illustrates the schematic diagram of a satellite onboard communications system. It consists of a user-link section in S-band with 30-m-class large reflector antenna, a digital section, and a feeder-link section. The digital section has a digital beamformer and channelizer (DBF/channelizer) for transmission and reception to meet the aforementioned requirements. To verify the required functionality for onboard satellite, a prototype user-link section (S-band radiating elements, diplexers, LNAs, SSPAs, D/Cs and U/Cs) and digital section (DBF/channelizer dedicated to sixteen elements and sixteen beams) has been developed and tested. Figure A.2 shows the externals of the small-scale models.

FIGURE A.1

Schematic diagram of satellite onboard communications system

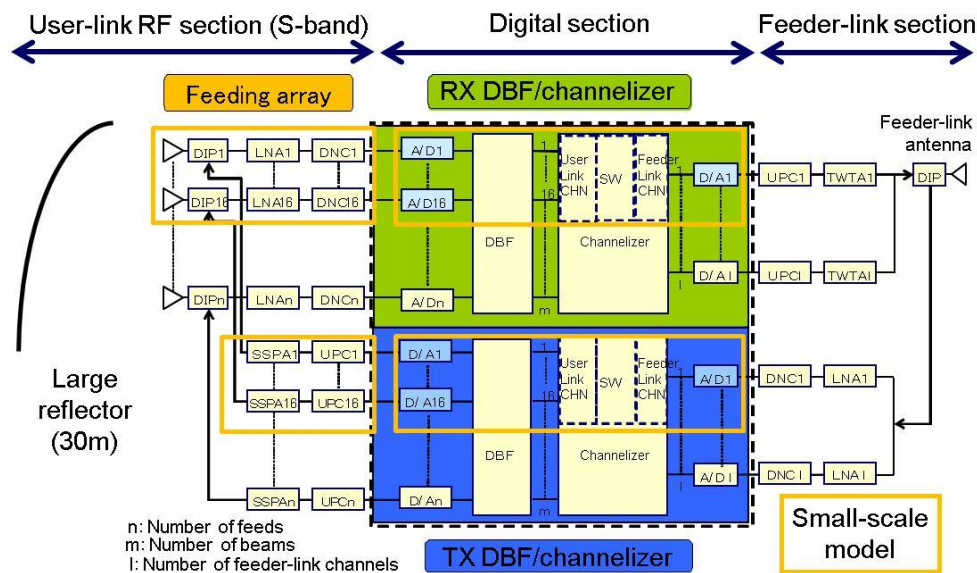
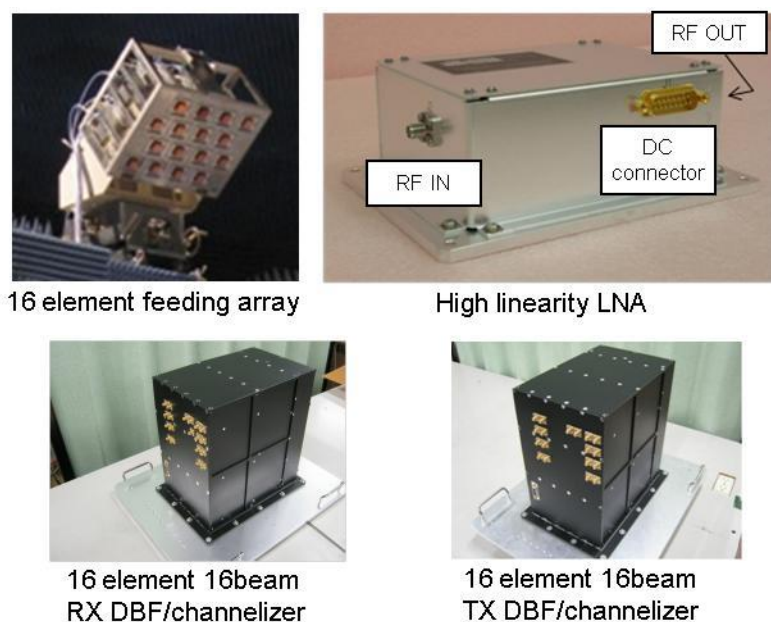


FIGURE A.2
Externals of small-scale models



2 Verification of multiple beamforming and sidelobe reduction

A prototype DBF/channelizer with sixteen-elements and sixteen-beams has been developed as part of a hundred-element and hundred-beam DBF/channelizer. As shown in Fig. A.3, the DBF, sixteen element feeding array, and a 3.3 m deployable mesh reflector were used for multi beam measurements in an anechoic chamber. Measurement of hundred beams was realized with multiple repetitive measurements of sixteen-beam DBF. Hundred beams with multi-colour frequency allocation (number of frequencies = seven) were allocated in the service area. Representative measured radiation patterns are shown in Fig. A.4. The result indicates that hundred beams are formed in the expected directions and that the measured radiation patterns agree with the calculated pattern. From these observations, the effectiveness of multi beam forming technology is confirmed.

FIGURE A.3
Externals of for multibeam measurement system

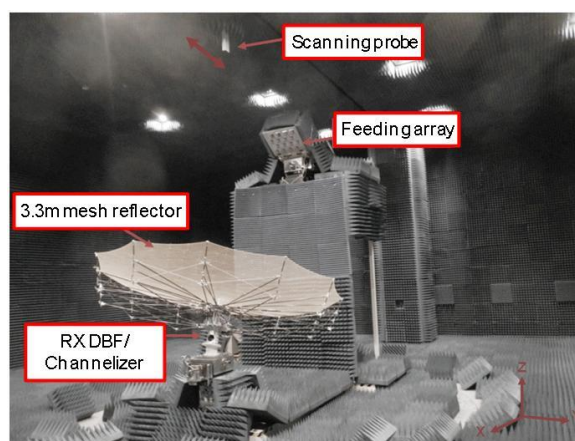
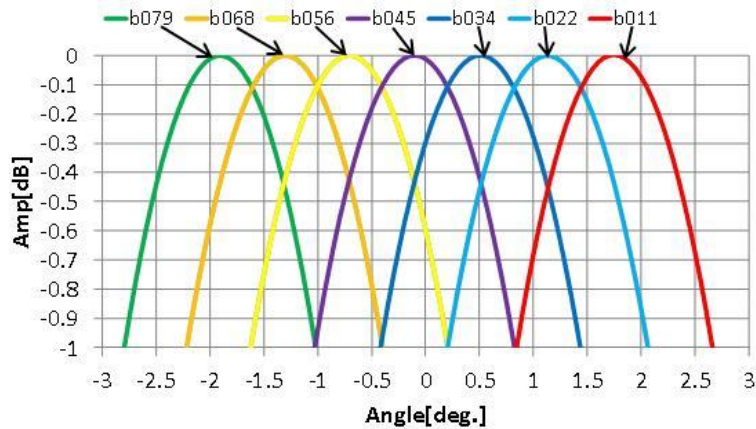


FIGURE A.4

Representative measured radiation patterns of hundred multibeams (seven beams)



To verify the effectiveness of sidelobe reduction in the satellite antenna for the integrated MSS system, the antenna sidelobe suppression test was conducted based on DBF weight control. The sixteen element DBF and feeding array was used for the measurement. Figure A.5 illustrates the verification process. Initially, a radiation pattern from a sixteen element feeding array with sixteen element DBF was measured using a near-field measurement system. The electromagnetic field on the virtual large reflector (27 m diameter) illuminated by the feeding array is then calculated using measured near-field data from the feeding array. Finally, the secondary radiation pattern is calculated using the electromagnetic field on the virtual large reflector. Four repetitive measurements of sixteen element DBF and feeding array were conducted to obtain the secondary radiation pattern of the reflector with 64 element feeding array. Excitation coefficient of DBF for the reduced sidelobe antenna is calculated and set to the DBF prior to the measurement. As shown in Fig. A.6, the evaluation results indicate that sidelobe reduction with 20 dB from peak gain of main beam was obtained.

FIGURE A.5

Verification process of sidelobe reduction

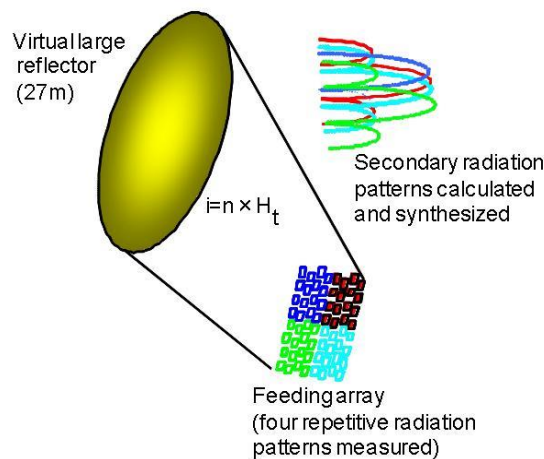
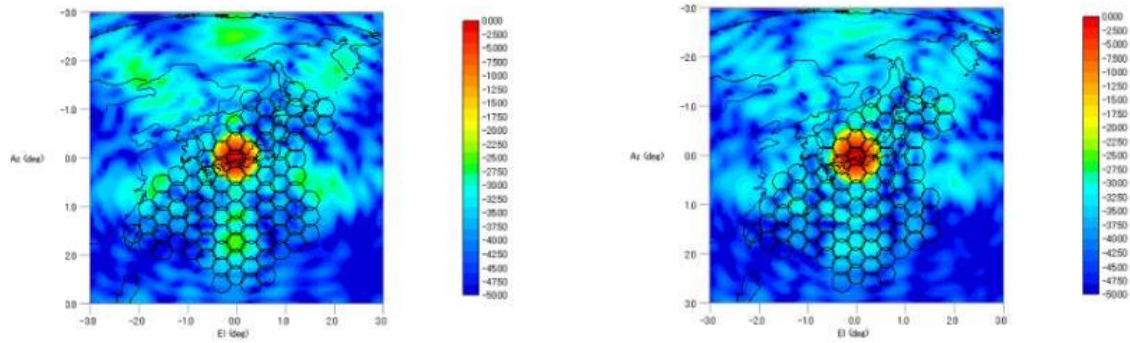


FIGURE A.6
Example results of sidelobe reduction test



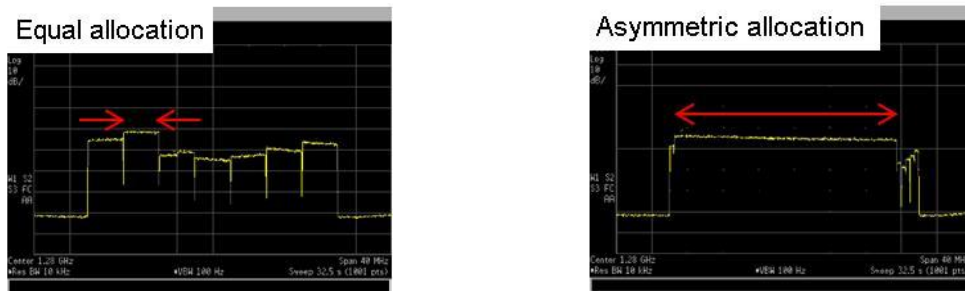
(a) Conventional pattern

(b) Low-sidelobe pattern

3 Verification of channelizing (resource re-allocation)

A channelizer achieves resource re-allocation functionality by dynamically changing frequency band allocation for each satellite beam. A performance test for the DBF/channelizer was carried out by coupling test of the transmitting and receiving DBF/channelizer. A resource allocation test was performed with two patterns of resource allocation states prepared for the evaluation; equal bandwidth allocation (4 MHz for each satellite beam) and wide bandwidth allocation to one particular satellite beam (25 MHz). As shown in the measured example of the test in Fig. A.7, it is observed that the beam bandwidth is changed to comply with each set of resource allocation patterns.

FIGURE A.7
Example data from resource allocation test



(a) Equal bandwidth allocation

(b) Wide bandwidth allocated to one satellite beam